Numerical Methods in Geotechnical Engineering – Schweiger (ed.)
© 2006 Taylor & Francis Group, London, ISBN 0-415-40822-9

A stress-strain integration algorithm for unsaturated soil elastoplasticity with automatic error control

W.T. Sołowski & D. Gallipoli
Durham University, Durham, United Kingdom

ABSTRACT: Stress-strain integration algorithms are a very important component in the development of finite element codes. The use of accurate, robust and fast stress-strain integration algorithms accounts for a significant part of the performance of a finite element code, especially when complex elasto-plastic constitutive models are used. This paper presents the formulation of an algorithm for the stress-strain integration of the Barcelona Basic Model, an elasto-plastic volumetric hardening constitutive model for unsaturated soils. The proposed algorithm is based on some earlier ideas of substepping explicit integration with automatic error control. Stress-strain integration in the plastic domain is performed by using an explicit algorithm which accuracy is improved by dividing the initial strain increment in a number of substeps. The number of substeps depends on an estimation of the integration error that is obtained by using a modified Euler procedure. The performance of the stress-strain algorithm is presented for different types of stress paths to assess its dependency on factors such as, for example, the initial size of the strain increment, the error tolerance and the initial stress state. A drift correction algorithm is also proposed and its influence on the results is evaluated.

1 INTRODUCTION

Elasto-plastic models for soils are often presented in the form of non-linear differential relationships between stress and strains that need to be integrated numerically for use within finite element codes. The robustness and efficiency of such numerical algorithms affects the overall performance of the code. Integration algorithms are divided into two broad groups: a) explicit algorithms where the integrated stress is obtained using the stiffness at the start of each integration step and b) implicit algorithms, where the stress increment is calculated using the stiffness at the end of the integration step (this requires an iterative approach as the values at the end of the step are initially unknown). Both methods are used in practice and have some advantages.

A general description of implicit algorithms may be found in Simo & Hughes (1998) where also an extensive list of references is available. Implicit algorithms for the integration of elasto-plastic models for saturated soils were developed, among others, by Borja & Lee (1990) and Borja (1991); recently new ideas were presented by Wang et al. (2004) and Foster et al. (2005). With reference to unsaturated soils, Vaunat et al. (2000) proposed an implicit integration algorithm including a return mapping scheme for the Barcelona Basic Model (BBM) of Alonso et al. (1990). Further implicit algorithms for unsaturated soil were proposed by Zhang et al. (2001) and Borja (2004).

Explicit algorithms have been often considered less efficient than implicit algorithms, although they are regarded as simpler to code and more generally applicable. A new class of explicit algorithms including error control based on a substepping method was proposed by Sloan (1987). Explicit algorithms with error control via substepping are now widely used and, especially for complicated elasto-plastic constitutive models, they are more robust and use less computational resources than implicit algorithms (see Potts & Zdravkovic 1999). Explicit algorithms using substepping have been constantly refined during past years and, recently, they have been applied to elasto-plastic models for unsaturated soils (e.g. Sheng et al. 2003a, b).

This paper presents an algorithm for the integration of BBM, however the concepts presented in the paper may be applied to any elasto-plastic model for unsaturated soils using two independent constitutive variables, such as net stress and suction. The integration of the stress-strain relationship is achieved explicitly via a substepping procedure to enforce error control.

For the sake of brevity the description of the purely elastic calculations is not presented in this paper and will be discussed in a future publication by the authors.

2 INTEGRATION OF ELASTO-PLASTIC STRAIN

2.1 *General remarks*

The stress-strain integration algorithm for unsaturated soils presented in this paper is similar to that proposed by Sheng et al (2003a). One important difference, however, is that, in the present work, the net stress and suction are treated as two separate constitutive variables (as in BBM) whereas Sheng et al. (2003a) use a single constitutive stress variable, which is defined as:

$$\boldsymbol{\sigma}' = \boldsymbol{\sigma}_{tot} - m\varphi(u_w)u_w = \boldsymbol{\sigma}_{tot} - \mathbf{m}\,\varphi(S_r)u_w \tag{1}$$

where $\boldsymbol{\sigma}'$ is the constitutive stress vector, $\boldsymbol{\sigma}_{tot}$ is the total stress vector, $\mathbf{m}^T = \{1,1,1,0,0,0\}$, $\varphi(S_r)$ is a constitutive stress parameter depending upon the degree of saturation S_r and u_w is the pore water pressure. The algorithm presented in this paper is instead used for integration of constitutive models for unsaturated soils depending on the net stress vector $\boldsymbol{\sigma}$, defined as $\boldsymbol{\sigma} = \boldsymbol{\sigma}_{tot} - \mathbf{m} \cdot u_a$ (where $\boldsymbol{\sigma}_{tot}$ is the total stress and u_a is the air pressure), as well as suction s, defined as $s = u_a - u_w$ (where u_a is the pore air pressure). These are also the standard constitutive variables used in various unsaturated soil models such as BBM.

The algorithm described here is explicit and uses a substepping procedure to achieve automatic error control during numerical integration according to the concepts first introduced by Sloan (1987). The algorithm integrates over an "extended" strain step $\{\Delta\boldsymbol{\varepsilon}_{tot}, \Delta s_{tot}\}$ incorporating the conventional strain increment vector $\Delta\boldsymbol{\varepsilon}_{tot}$ as well as the increment of suction Δs_{tot}. These increments are automatically divided into a number of substeps, small enough to ensure the desired integration accuracy. It is also assumed that the change of suction in each substep Δs is proportional to the change of strain $\Delta\boldsymbol{\varepsilon}$, i.e. $\Delta s/\Delta s_{tot} = \Delta\varepsilon_{ij}/\Delta\varepsilon_{ij,tot}$. The integration error in each substep is estimated as the difference between the two stress increments calculated by using the elasto-plastic stiffness matrix corresponding to the stress states at the beginning and the end of the substep respectively. Based on such estimate of the error, the size of the next substep is calculated.

2.2 *Integration of elasto-plastic substep*

In each substep involving elasto-plastic deformation, the net stress increment $\Delta\boldsymbol{\sigma}$ is calculated from the strain substep $\Delta\boldsymbol{\varepsilon} = \Delta T^*\Delta\boldsymbol{\varepsilon}_{tot}$ and the suction substep $\Delta s = \Delta T^*\Delta s_{tot}$ (ΔT is a scalar). The yield function F and plastic potential G are defined in terms of the net stress $\boldsymbol{\sigma}$, suction s and hardening parameter p_0^*:

$$F = F(\boldsymbol{\sigma}, s, p_0^*) = 0 \tag{2}$$

$$G = G(\boldsymbol{\sigma}, s, p_0^*) = 0 \tag{3}$$

The plastic strain increment is given by:

$$d\boldsymbol{\varepsilon}^{pl} = \lambda\frac{\partial G(\boldsymbol{\sigma}, s, p_0^*)}{\partial\boldsymbol{\sigma}} \tag{4}$$

where λ is the plastic multiplier. The volumetric plastic strain increment $d\varepsilon_v^{pl} = d\varepsilon_{11}^{pl} + d\varepsilon_{22}^{pl} + d\varepsilon_{33}^{pl}$ is related to a change of the hardening parameter p_0^* according to the following equation:

$$dp_0^* = \frac{\partial p_0^*}{\partial\varepsilon_v^{pl}}d\varepsilon_v^{pl} \tag{5}$$

The consistency condition to be satisfied by all incremental quantities is:

$$dF = \left(\frac{\partial F}{\partial\boldsymbol{\sigma}}\right)^T d\boldsymbol{\sigma} + \left(\frac{\partial F}{\partial s}\right)^T ds + \left(\frac{\partial F}{\partial p_0^*}\right)^T dp_0^* = 0 \tag{6}$$

The differential form of the stress–strain relationship for BBM, is given by:

$$d\boldsymbol{\sigma} = \mathbf{D}^{el}d\boldsymbol{\varepsilon}^{el} = \mathbf{D}^{el}(d\boldsymbol{\varepsilon} - d\boldsymbol{\varepsilon}^{pl} - \frac{1}{3}\mathbf{m}\frac{\kappa_s ds}{p_{at} + s}) \tag{7}$$

where $\mathbf{D}^{el}$ is the elastic tangent matrix calculated at the beginning of the increment, $d\boldsymbol{\varepsilon}$ is the strain increment, $d\boldsymbol{\varepsilon}^{pl}$ is the plastic component of the strain increment, κ_s is the swelling index associated to suction change and p_{at} is atmospheric pressure. Introducing (4) into (7) gives:

$$d\boldsymbol{\sigma} = \mathbf{D}^{el}d\boldsymbol{\varepsilon} - \lambda\mathbf{D}^{el}\frac{\partial G(\boldsymbol{\sigma}, s, p_0^*)}{\partial\boldsymbol{\sigma}} - \frac{1}{3}\mathbf{D}^{el}\mathbf{m}\frac{\kappa_s ds}{p_{at} + s} \tag{8}$$

After introducing (8) into (6) and noting that transposition of a scalar variable coincides with the scalar variable itself, the following relationship is obtained:

$$\left(\mathbf{D}_{el}d\boldsymbol{\varepsilon} - \mathbf{D}_{el}\frac{\partial G(\boldsymbol{\sigma}, s, p_0^*)}{\partial\boldsymbol{\sigma}}\lambda - \frac{1}{3}\mathbf{D}_{el}\mathbf{m}\frac{\kappa_s ds}{p_{at} + s}\right) \cdot \left(\frac{\partial F}{\partial\boldsymbol{\sigma}}\right)^T + \frac{\partial F}{\partial s}ds + \frac{\partial F}{\partial p_0^*}dp_0^* = 0 \tag{9}$$

As dp_0^* is a function of the plastic volumetric strain increment as indicated in (5), then:

$$\left(\frac{\partial F}{\partial p_0^*}\right)dp_0^* = \left(\frac{\partial F}{\partial p_0^*}\right)\left(\frac{\partial p_0^*}{\partial\varepsilon_v^{pl}}\right)d\varepsilon_v^{pl} \tag{10}$$

and, after expressing $d\varepsilon_v^{pl}$ as:

$$d\varepsilon_v^{pl} = \sum_{i=1}^{3} d\varepsilon_{ii}^{pl} = \lambda \mathbf{m}^T \left(\frac{\partial G(\boldsymbol{\sigma}, s, p_0^*)}{\partial \boldsymbol{\sigma}} \right) \tag{11}$$

the following result is obtained:

$$\left(\frac{\partial F}{\partial p_0^*} \right) dp_0^* = \lambda \left(\frac{\partial F}{\partial p_0^*} \right) \left(\frac{\partial p_0^*}{\partial \varepsilon_v^{pl}} \right) \mathbf{m}^T \left(\frac{\partial G(\boldsymbol{\sigma}, s, p_0^*)}{\partial \boldsymbol{\sigma}} \right) \tag{12}$$

Introducing (12) into (9), λ can be expressed as:

$$\lambda = \frac{\mathbf{a}^T \mathbf{D}^{el} d\boldsymbol{\varepsilon} + \left[c - \mathbf{a}^T \mathbf{D}^{el} \mathbf{b} \right] ds}{\mathbf{a}^T \mathbf{D}^{el} \mathbf{g} - d} \tag{13}$$

where:

$$\frac{\partial F}{\partial \boldsymbol{\sigma}} = \mathbf{a}, \quad \frac{1}{3} \mathbf{m} \frac{\kappa_s}{p_{at} + s} = \mathbf{b}, \quad \frac{\partial F}{\partial s} = c,$$
$$\frac{\partial F}{\partial p_0^*} \frac{\partial p_0^*}{\partial \varepsilon_v^{pl}} \mathbf{m}^T \frac{\partial G}{\partial \boldsymbol{\sigma}} = d, \quad \frac{\partial G}{\partial \boldsymbol{\sigma}} = \mathbf{g}$$

In the integration algorithm the infinitesimal increments in the above equations (densoted by "d") are approximated with finite increments (denoted by "Δ"). Please note that equation (13) is different from the corresponding equation given in Sheng et al. (2003a) due to different assumptions made about the constitutive variables, as previously discussed.

Having computed the plastic multiplier λ, the stress increment is calculated from (8), the volumetric plastic strain increment is calculated from (11) and the hardening parameter increment is obtained from (5).

2.3 *Evaluation of integration error*

In each substep the algorithm calculates: a) two values of the stress increment, $\Delta\boldsymbol{\sigma}_1$ and $\Delta\boldsymbol{\sigma}_2$, b) two values of volumetric plastic strain increment $\Delta\varepsilon_v^{pl}{}_1$ and $\Delta\varepsilon_v^{pl}{}_2$ and c) two values of the hardening parameter increment Δp_{01}^* and Δp_{02}^*.

The increments with subscript equal to 1 are calculated according to the equations given in the previous section and using values of the stress and hardening parameter at the start of the increment:

$$\begin{aligned} \Delta\boldsymbol{\sigma}_1 &= \Delta\boldsymbol{\sigma}_1 \left(\Delta\boldsymbol{\varepsilon}, \Delta s, \boldsymbol{\sigma}_0, p_0^* \right) \\ \Delta p_{0,1}^* &= \Delta p_{0,1}^* \left(\Delta\boldsymbol{\varepsilon}, \Delta s, \boldsymbol{\sigma}_0, p_0^* \right) \end{aligned} \tag{14}$$

The increments with subscript equal to "2" are calculated according to the same equations but using values of the stress and hardening parameter at the end of the increment. Note that the values at the end of the increment are calculated by using the increments from equation (14):

$$\begin{aligned} \Delta\boldsymbol{\sigma}_2 &= \Delta\boldsymbol{\sigma}_2 \left(\Delta\boldsymbol{\varepsilon}, \Delta s, \boldsymbol{\sigma}_0 + \Delta\boldsymbol{\sigma}_1, p_0^* + \Delta p_{0,1}^* \right) \\ \Delta p_{0,2}^* &= \Delta p_{0,2}^* \left(\Delta\boldsymbol{\varepsilon}, \Delta s, \boldsymbol{\sigma}_0 + \Delta\boldsymbol{\sigma}_1, p_0^* + \Delta p_{0,1}^* \right) \end{aligned} \tag{15}$$

Equations (14) and (15) define an interval of values containing the exact integration of these increments. The best estimates of the stress increment $\Delta\boldsymbol{\sigma}$ and the hardening parameter increment Δp_0^* are taken as the average of the corresponding two values defined above:

$$\Delta\boldsymbol{\sigma} = \frac{\Delta\boldsymbol{\sigma}_1 + \Delta\boldsymbol{\sigma}_2}{2} \tag{16}$$

$$\Delta p_0^* = \frac{\Delta p_{0,1}^* + \Delta p_{0,2}^*}{2} \tag{17}$$

The maximum integration error for the stress increment is therefore calculated from the previous expressions for each of the stress components as:

$$E_{ij} = 0.5 \left| \Delta\sigma_{ij,2} - \Delta\sigma_{ij,1} \right| \quad i, j = 1,2,3 \tag{18}$$

The relative error R_{ij} is defined as:

$$R_{ij} = \frac{E_{ij}}{\left| \Delta\sigma_{ij} \right|} \quad i, j = 1,2,3 \tag{19}$$

This is not sufficient to ensure that the relative error in shear stress q, crucial for soil behaviour, is limited. This is why also E_q and R_q is defined:

$$E_q = \max\left(\left| q_1 - q_{mid} \right|, \left| q_2 - q_{mid} \right| \right), \quad R_q = \frac{E_q}{q_{mid} - q_0} \tag{20}$$

In the formula above q_0 is the initial shear stress corresponding to the stress state $\boldsymbol{\sigma}_0$ and q_1, q_2, q_{mid} are shear stresses calculated for corresponding stress states $\boldsymbol{\sigma}_0 + \Delta\boldsymbol{\sigma}_1$, $\boldsymbol{\sigma}_0 + \Delta\boldsymbol{\sigma}_2$, and $\boldsymbol{\sigma}_0 + 0.5(\Delta\boldsymbol{\sigma}_1 + \Delta\boldsymbol{\sigma}_2)$. In the calculations the highest value of R is used:

$$R = \max\left(R_{11}, R_{22}, R_{33}, R_{12}, R_{13}, R_{23}, R_q \right) \tag{21}$$

Equations (18) and (19) provide an estimate of the maximum potential error occurring during integration; however the actual error is usually significantly smaller than these values.

Control of the integration error is enforced by imposing that R in equation (19) is equal or smaller

than a user defined substep tolerance SSTOL. If R > SSTOL, the current substep is rejected. Regardless of whether the current substep is accepted or rejected, a new substep size is calculated by the algorithm with the coefficient ΔT_{new} given by:

$$\Delta T_{new} = \beta \Delta T \tag{22}$$

where ΔT defines the current size of the substep and β is a coefficient; β is smaller than 1, if the step is rejected, or equal/greater than 1, if the step is accepted. In this way the substep size is continuously adapted to enforce a magnitude of the maximum possible relative error R close to SSTOL.

The error estimate associated with the new substep size can be approximated as:

$$E_{new} = \beta^2 E \tag{23}$$

Substituting equation (19) into equation (23) and imposing that the maximum relative error in the next substep is equal to the tolerance SSTOL, it is possible to calculate an approximated value of β as:

$$\beta \approx \sqrt{\frac{SSTOL}{R}} \tag{24}$$

Equation (24) relies on the approximation $\Delta\boldsymbol{\sigma} = \Delta\boldsymbol{\sigma}_{new}$ Because of this approximation, β is usually further reduced by a user defined scalar factor ξ as:

$$\beta = \xi \sqrt{\frac{SSTOL}{R}} \tag{25}$$

In the subsequent examples a value $\xi = 0.9$ is used.

2.4 Drift correction

Because of the approximation involved in the use of explicit integration, the stress state at the end of each substep does not lie on the yield locus. This phenomenon is known as yield surface drift and it requires a numerical correction to enforce consistency. Drift correction tends to become less of an issue as the tolerance used for the control of the integration error becomes stricter. The drift correction technique used in this work is similar to that advocated by Potts & Zdravkovic (1999) for saturated soil models.

The drift correction procedure is used when, after a successful substep (i.e. a substep where the integration error R is smaller or equal than the tolerance SSTOL), the stress state does not lie on the yield locus within a set tolerance. In the present algorithm a normalized yield function is used for BBM, similarly to the normalized function proposed by Sheng et al. (2000) for the Cam-clay model. Employing a normalized yield locus ensures that the set tolerance is independent of the magnitude of the stress state.

Before integration, the initial stress state $\boldsymbol{\sigma}_A$ lies on the yield locus at point A in the stress space and therefore $F(\boldsymbol{\sigma}_A, s_A, p^*_{0A}) = 0$. After calculating the stress increase $\Delta\boldsymbol{\sigma}$, as explained in the previous section, the stress state changes to $\boldsymbol{\sigma}_B = \boldsymbol{\sigma}_A + \Delta\boldsymbol{\sigma}$ moving to point B of the stress space. and is not any longer on the yield locus, i.e. $F(\boldsymbol{\sigma}_B, s_B, p^*_{0B}) \neq 0$. The drift correction algorithm imposes a change of the elastic strain $\Delta\boldsymbol{\varepsilon}^e$ (by maintaining unchanged the strain $\Delta\boldsymbol{\varepsilon}$, i.e. $\Delta\boldsymbol{\varepsilon}^e = -\Delta\boldsymbol{\varepsilon}^{pl}$), which results in the correction of the stress state to point C lying on the yield locus. The yield locus equation after correction will therefore be:

$$F(\boldsymbol{\sigma}_C, s, p^*_{0C}) = F(\boldsymbol{\sigma}_B + \Delta\boldsymbol{\sigma}, s, p^*_{0B} + \Delta p^*_0) = 0 \tag{26}$$

where $\Delta\boldsymbol{\sigma}$ and Δp^*_0 are the corrections to the stress state and hardening parameter respectively and no correction to suction is applied as explained below.

After expanding (24) in Taylor series we obtain:

$$F(\boldsymbol{\sigma}_C, s, p^*_{0C}) = F(\boldsymbol{\sigma}_B, s, p^*_{0B}) + \left(\frac{\partial F}{\partial \boldsymbol{\sigma}}\right)^T \Delta\boldsymbol{\sigma} + \frac{\partial F}{\partial s}\Delta s + \frac{\partial F}{\partial p^*_0}\Delta p^*_0 + \ldots \tag{27}$$

where the stress change $\Delta\boldsymbol{\sigma}$ is:

$$\Delta\boldsymbol{\sigma} = \Delta\boldsymbol{\sigma}(\Delta\boldsymbol{\varepsilon}^{el}) = \mathbf{D}^{el}\Delta\boldsymbol{\varepsilon}^{el} = -\mathbf{D}^{el}\Delta\boldsymbol{\varepsilon}^{pl} = -\mathbf{D}^{el}\lambda\frac{\partial G}{\partial \boldsymbol{\sigma}} \tag{28}$$

After substituting (28) and (13) into (26), neglecting second order terms and above and noticing that the change of suction Δs is equal to zero (as suction change is proportional to the variation of strain $\Delta\boldsymbol{\varepsilon}$ which remains unchanged) the following expression for λ is obtained:

$$\lambda = \frac{F(\boldsymbol{\sigma}_B, s, p^*_{0B})}{\left(\frac{\partial F}{\partial \boldsymbol{\sigma}}\right)^T \mathbf{D}^{el}\frac{\partial G}{\partial \boldsymbol{\sigma}} - \frac{\partial F}{\partial p^*_0}\frac{\partial p^*_0}{\partial \varepsilon^{pl}}\mathbf{m}^T\frac{\partial G(\boldsymbol{\sigma}, s, p^*_0)}{\partial \boldsymbol{\sigma}}} \tag{29}$$

The stress state in point C is then equal to:

$$\boldsymbol{\sigma}_C = \boldsymbol{\sigma}_B - \lambda\mathbf{D}^{el}\frac{\partial G}{\partial \boldsymbol{\sigma}} \tag{30}$$

In the unlikely situation when, after the first correction, the stress state still lies outside the yield locus, the above algorithm is performed again until the

stress state is mapped back onto the yield locus within the set tolerance. The derivatives and stiffness matrix appearing in the above equations may be calculated either at point A or at point B. The effect of calculating those quantities at different points of the stress path during each substep is discussed later in the paper.

3 VALIDATION OF PROPOSED INTEGRATION ALGORITHM

3.1 *Overview*

To validate the algorithm results from number of simple cases with existing theoretical solution were compared to the solutions given by the algorithm. In all the cases a Barcelona Basic Model (BBM) developed by Alonso et al. (1990) was used. Although the theoretical solution (see equation 14) allows for a non-associated flow rule, as originally proposed by Alonso et al. (1990), in validation of the code and in all examples an associated flow rule was used. The parameters of the model in each case were the same: Shear Modulus (constant) G = 20 MPa, elastic stiffness parameter for changes in net mean stress $\kappa = 0.02$, elastic stiffness parameter for changes in suction $\kappa_s = 0.008$, atmospheric pressure $p_{atm} = 100{,}000$ Pa, parameter describing the increase in cohesion with suction k = 0.6, stiffness parameter for changes in net mean stress for virgin states of the soil (with suction s = 0) $\lambda(0) = 0.2$, parameter defining the maximum increase of soil stiffness with suction $\beta = 0.00001$, reference stress $p_c = 10{,}000$ Pa, starting specific volume at means stress $p = p^c$ and suction s = 0 N(0) = 1.9, critical state line slope M = 0.5. The initial preconsolidation stress for saturated condition p_0^* was set to 200,000 Pa and initial suction s used was equal to 100,000 Pa.

3.2 *Test case 1 – isotropic loading of a sample subjected to drying*

The test simulates isotropic loading of a preconsolidated and partially unloaded sample. The sample was initially in isotropic stress state with the mean stress p = 350,000 Pa. The sample was subjected to strain change $\Delta\varepsilon = \{0.05,0.05,0.05,0,0,0\}$ and suction increase $\Delta s = 100{,}000$ Pa. Created algorithm showed good convergence to the theoretical solution. (please refer to Fig. 1 & Table 1)

3.3 *Test case 2 – oedometric test at variable suction*

The test simulates oedometric test with drying of a sample during a test. The sample was in isotropic stress state at the beginning of the test with mean stress p = 350,000 Pa. Sample then was subjected to strain change $\Delta\boldsymbol{\varepsilon} = \{0.05,0,0,0,0,0\}$ and suction increase $\Delta s = 100{,}000$ Pa. Again a very good agreement of the data from the algorithm with the theoretical solution was found (see Fig. 2 and Table 1)

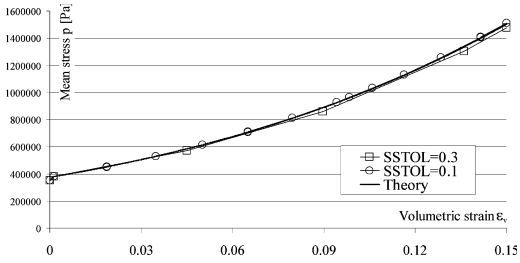

Figure 1. Comparison of the algorithm solutions obtained for different values of substep accuracy SSTOL with the theoretical solution (no drift correction).

Table 1. Comparison of drift correction algorithms.

Test case	Integration at:	SSTOL value [%]	Number of steps	Number of drift corrections	Relative Error (comparing to the theory), for mean stress p and shear stress q [%]
1	A	30	4	36	0.252*
1	B	30	28	177	1.006*
1	–	30	4	–	2.59*
1	A	10	10	109	0.669*
1	B	10	10	175	0.724*
1	–	10	10	–	0.490*
1	A	1	104	1040	0.0920*
1	B	1	104	1137	0.0929*
1	–	1	104	–	0.0274*
1	A	0.1	1043	6543	0.009229*
1	B	0.1	1043	6598	0.009238*
1	–	0.1	1043	–	0.002744*
2	A	30	30	161	0.0581/1.152
2	B	30	30	180	0.0451/1.059
2	–	30	26	–	0.570/0.555
2	A	10	59	286	0.0124/0.472
2	B	10	59	309	0.0105/0.465
2	–	10	56	–	0.292/0.0922
2	A	1	423	1306	4.22E-04/0.0585
2	B	1	423	1338	4.88E-04/0.0585
2	–	1	419	–	0.0414/0.00187
2	A	0.1	4026	4432	2.4E-05/0.00647
2	B	0.1	4026	4436	2.5E-05/0.00647
2	–	0.1	4022	–	0.00499/6.0E-04

*for test case 1 only error in p is given as q = 0.

4 INFLUENCE OF DRIFT CORRECTION ALGORITHM

The choice of the drift correction algorithm influences the accuracy of the result. As mentioned in

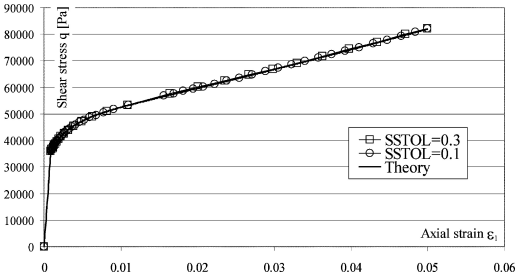

Figure 2. Comparison of the theoretical ε-q path with the solutions from the algorithm for different values of substep tolerance SSTOL (no drift correction).

point 2.4 two implementation of the algorithm are possible. In one case the derivatives and the elastic matrix are calculated at the beginning of the substep (point A), in the other in forbidden space at point B (neither solution is rigorous). To check the influence of the drift correction algorithm, both cases were implemented. Results show little difference, but in extreme cases when, because of crude accuracy, very few steps accompanied by multiple iterations of drift correction algorithm were computed (see Table 1). In such case calculating all the derivatives at point A was often advantageous and resulted in more accurate results and/or in less iteration needed to converge to the yield locus. Such uncommon amounts of iterations of drift correction algorithm were performed because of artificially set very strict tolerance for a stress state to be considered as being on the yield locus. These results are in a good agreement with data presented by Potts & Zdravkovic (1999). In table 1 are also included the values obtained without the drift correction algorithm (indicated with "–"). As the correction of the stress state in the algorithm proposed is artificial and not rigorous, although in result the stress state is returned back to the yield surface, in some cases the overall accuracy may be decreased.

5 CONCLUSIONS

The paper presents an algorithm for the numerical integration of the differential stress-strain relationship in BBM. The algorithm uses explicit integration and incorporates a substepping procedure for controlling the integration error. The methodology outlined in the present paper can also be applied to other unsaturated elasto-plastic models expressed in terms of two different constitutive variables, e.g. net stress and suction.

The difficulties in estimating the numerical integration error have been highlighted. It has been shown that the bound (maximum) error, as in equation (19), significantly overestimates the actual error and therefore the level of accuracy is considerably greater (see also Gear 1971) than the tolerance SSTOL. This implies that the algorithm uses a larger number of substeps than what is required to achieve accuracy equal to SSTOL.

Different implementations of the drift correction algorithms have also been presented and discussed. It might seem somewhat surprising that in some cases (see Table 1) the use of the drift correction algorithm reduces the integration accuracy with respect to similar cases when no drift correction is applied. However, in most examples (including some not presented in this paper) the drift correction procedure proved to be useful and helped to improve integration accuracy. The examples presented here are rather basic which may explain why the algorithm without the drift correction works equally well. Results also show that similar levels of accuracy are obtained regardless whether the stiffness and the derivatives in the drift correction algorithm are calculated at the end or at the beginning of the substep.

The main advantage of the proposed algorithm lies in controlling the numerical integration error for BBM below a given tolerance set by the user. The algorithm also appears to be robust and yields accurate results for different types of stress paths (some not presented in this paper). Current research at Durham University is focusing on the application of the algorithm to advanced constitutive models proposed recently to link the mechanical behaviour to the retention properties of the soil, e.g. Gallipoli et al. (2003).

ACKNOWLEDGMENTS

Authors gratefully acknowledge funding by the European Commission through the MUSE Research Training Network, contract: MRTN-CT-2004-506861

REFERENCES

Alonso, E.E., Gens, A. & Josa, A. 1990. A constitutive model for partially saturated soils. Géotechnique 40(3): 405–430.

Borja, R.I. & Lee, S.R. 1990. Cam-Clay plasticity. Part I: Implicit integration of elastoplastic constitutive relations, Comput. Methods Appl. Mech. Engg. 78(1): 49–72.

Borja, R.I. 1991. Cam-Clay plasticity, Part II: Implicit integration of constitutive equation based on a nonlinear elastic stress predictor. Comput. Methods Appl. Mech. Engrg. 88(2): 225–240.

Borja, R.I. 2004. Cam-Clay plasticity. Part V: A mathematical framework for three-phase deformation and strain localization analyses of partially saturated porous media. Comput. Methods Appl. Mech. Engg. 193(48–51): 5301–5338.

Foster, C.D., Regueiro, R.A., Fossum, A.F. & Borja, R.I. 2005. Implicit numerical integration of a three-invariant,

isotropic/kinematic hardening cap plasticity model for geomaterials. Comput. Methods Appl. Mech. Engrg. 194: 5109–5138.

Gallipoli, D., Gens, A., Sharma, R. & Vaunat, J. 2003. An elastoplastic model for unsaturated soil incorporating the effects of suction and degree of saturation on mechanical behaviour. Géotechnique 53(1):123–135.

Gear, W.G. (1971). Numerical initial value problems in ordinary differential equations. Englewood Cliffs, New Jersey USA: Prentice Hall Inc.

Potts, D.M. & Zdravkovic, L. 1999. Finite element analysis in geotechnical engineering. Theory. London: Thomas Telford Publishing.

Sheng, D., Sloan, S.W., Gens, A. & Smith, D.W. 2003a. Finite element formulation and algorithms for unsaturated soils. Part I: Theory. Int. J. Numer. Anal. Meth. Geomech, 27: 745–765.

Sheng, D., Sloan, S.W., Gens, A. & Smith, D.W. 2003b. Finite element formulation and algorithms for unsaturated soils. Part II: Verification and application. Int. J. Numer. Anal. Meth. Geomech, 27: 767–790.

Sheng, D, Sloan, S.W. & Yu, H.S. 2000. Aspects of finite element implementation of critical state models. Computational Mechanics 26: 185–196.

Simo, J.C. & Hughes, T.J.R. 1998. Computational inelasticity. New York: Springer.

Sloan, S.W. 1987. Substepping schemes for the numerical integration of elastoplastic stress-strain relations. Int. J. Numer. Methods Eng. 24: 893–911.

Sloan, S.W., Abbo, A. J. & Sheng, D. 2001. Refined explicit integration of elastoplastic models with automatic error control. Engineering Computations 18(1/2): 121–154.

Vaunat, J., Cante, J.C., Ledesma, A. & Gens, A. 2000. A stress point algorithm for an elastoplastic model in unsaturated soils. International Journal of Plasticity, 16: 121–141.

Wang, X., Wang, L.B. & Xu, L.M. 2004. Formulation of the return mapping algorithm for elastoplastic soil models, Computers and Geotechnics 31: 315–338.

Zhang, H.W., Heeres, O.M., de Borst, R. & Schrefler, B.A. 2001. Implicit integration of a generalized plasticity constitutive model for partially saturated soil. Engineering Computations, Vol. 18(1/2): 314–336.